COPYRIGHT 2026 © BY THE ARCHIVES OF BONE AND JOINT SURGERY

PERSPECTIVE

Imaging Atlas of Osseous Pathology in the Ankle and Foot

Pegah Sahafi, MD; Mohammad Hadi Samadi, MD; Alireza Mousavian, MD; Vahid Reza Dabbagh Kakhki, MD; Ramin Sadeghi, MD

Research performed at Nuclear Medicine Department, Qaem Hospital, Mashhad, Iran

Received: 11 January 2026 *Accepted: 02 March 2026*

Abstract

This study aimed to characterize the imaging patterns of osseous pathologies of the ankle and foot using bone scintigraphy and 99mTc-MDP SPECT/CT. Illustrative cases of traumatic, degenerative, infectious, metabolic, and neoplastic lesions were evaluated. The findings of bone scintigraphy and SPECT/CT were compared with those of radiography, CT, and MRI. SPECT/CT improved the localization and characterization of lesions in the anatomically complex ankle–foot region. Distinguishing normal from abnormal uptake patterns helped reduce potential misdiagnoses. 99mTc-MDP bone scintigraphy and SPECT/CT are valuable imaging modalities for detecting and characterizing ankle and foot pathologies, enhancing diagnostic confidence and guiding clinical management.

Level of evidence: V

Keywords: Ankle and foot pathology, Bone tumors, Bone scan, Scintigraphy, SPECT/CT, 99mTc-MDP,

Introduction

Osseous pathologies of the ankle and foot present significant diagnostic challenges due to their complex anatomy and often nonspecific clinical manifestations. Accurate evaluation requires thorough familiarity with regional anatomy and the characteristic imaging patterns of various disorders. Hybrid imaging modalities, particularly 99mTc-MDP SPECT/CT, integrate metabolic and anatomical information, thereby improving lesion localization, characterization, and differentiation between benign and malignant processes. This atlas presents representative cases of traumatic, degenerative, infectious, and neoplastic conditions affecting the ankle and foot, highlighting characteristic nuclear medicine findings and their correlation with radiography, CT, and MRI. Recognition of normal variants, growth-related tracer uptake, and disease-specific imaging patterns is essential to optimize diagnostic accuracy and guide clinical management.

Materials and Methods

A series of representative traumatic, degenerative, infectious, metabolic, and neoplastic lesions was examined. Imaging findings from bone scintigraphy and SPECT/CT were systematically correlated with those of radiography, computed tomography (CT), and magnetic resonance imaging (MRI).

Physiologic physeal tracer uptake in the calcaneus and distal fibula of a young boy. Symmetrical, linear uptake is typical; asymmetry or focal deviation may suggest underlying pathology [Figure 1].

Accessory ossicles in two patients. (A) Bilateral accessory navicular bones (tibiale externum) in a 45-year-old patient with medial left ankle and foot pain. This ossicle represents a prominent accessory bone located along the medial aspect of the navicular bone [Figure 2A]. (B) Bipartite hallux sesamoid (arrows) and a fracture of the left third metatarsal in a 53-year-old patient following intense exercise [Figure 2B]. Bipartite sesamoids represent normal variants

Corresponding Author: Ramin Sadeghi, Nuclear Medicine Research Center, Mashhad University of Medical Sciences, Mashhad, Iran

Email: sadeghir@mums.ac.ir

THE ONLINE VERSION OF THIS ARTICLE ABJS.MUMS.AC.IR

Arch Bone Jt Surg. 2026;14(4):321-328 Doi: 10.22038/ABJS.2026.93807.4233 http://abjs.mums.ac.ir

Copyright © 2026 Mashhad University of Medical Sciences. This work is licensed under a Creative Commons Attribution-Noncommercial 4.0 International License https://creativecommons.org/licenses/by-nc/4.0/deed.en

resulting from incomplete ossification.[1]

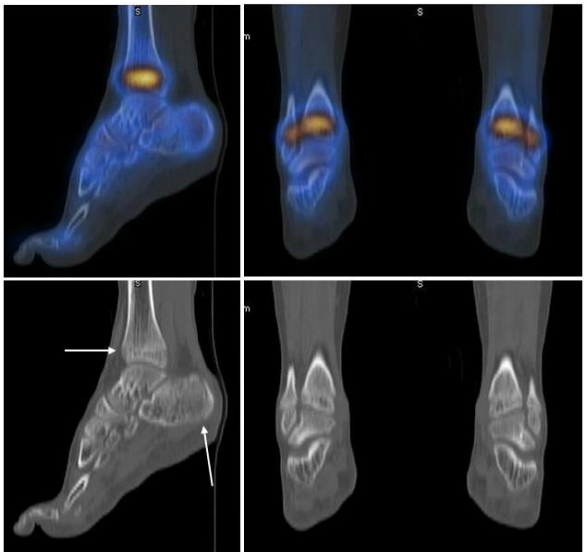

Figure 1. *Normal physeal uptake in the calcaneus* and fibula (arrows)

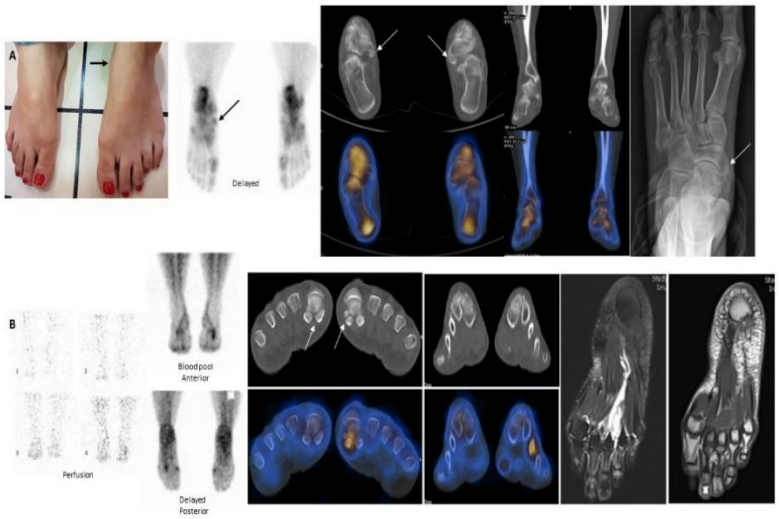

Figure 2. (A) Bilateral accessory navicular; (B) bipartite hallux sesamoid (arrows) With an associated fracture of the left third metatarsal

The two most common types of tarsal coalition are talocalcaneal and calcaneonavicular coalitions. In a talocalcaneal coalition, any or all facets of the subtalar joint (anterior, middle, and posterior) may be involved, and the condition is bilateral in most patients. (A) Bilateral talocalcaneal coalition in a 19-year-old patient presenting with medial midfoot pain during exercise [Figure 3A]. (B) Calcaneonavicular coalition in a 45-year-old man with chronic ankle pain [Figure 3B].

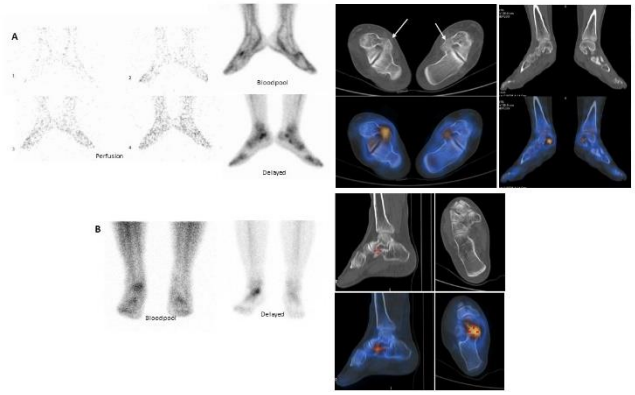

Figure 3. (A) bilateral talocalcaneal coalition in a young patient; (B) calcaneonavicular coalition in a man with chronic ankle pain

Fractures in two separate patients demonstrating increased ^99mTc-MDP uptake in all phases of bone scintigraphy. (A) Talus fracture with a visible fracture line and adjacent bone marrow edema on MRI [Figure 4A]. (B) Fracture of the fifth metatarsal [Figure 4B].

Figure 4. Fractures: (A) talus fracture with a visible fracture line and associated bone marrow edema on MRI; (B) fifth metatarsal fracture

Impingement syndrome is characterized by compression of soft tissues or osseous structures. It may occur in the anterior ankle [Figure 5A] or posterior ankle [Figure 5B]. Posterior impingement (os trigonum syndrome) is frequently associated with the presence of an os trigonum (arrow).[2]

Osteochondral lesions of the talus in two patients, demonstrating increased blood-pool and delayed-phase tracer uptake. These lesions result from injury to the articular cartilage and subchondral bone, often secondary to trauma, with possible fragment detachment [Figure 6].[3]

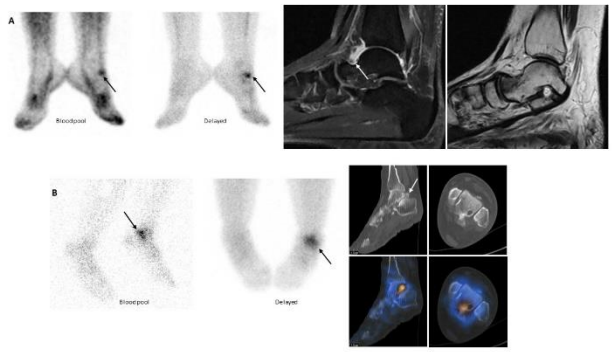

Figure 5. Impingement syndrome involving the anterior (A) and posterior (B) ankle regions

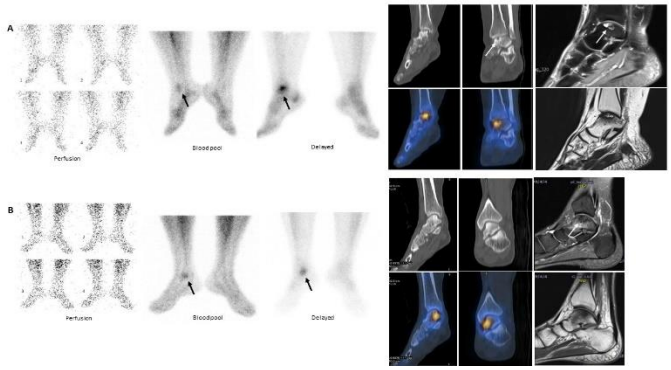

Figure 6. Osteochondral lesions of the talus in two separate patients

Plantar fasciitis of the left foot in a soldier, demonstrating increased uptake at the calcaneal origin of the plantar fascia, often associated with heel spur formation [Figure 7].

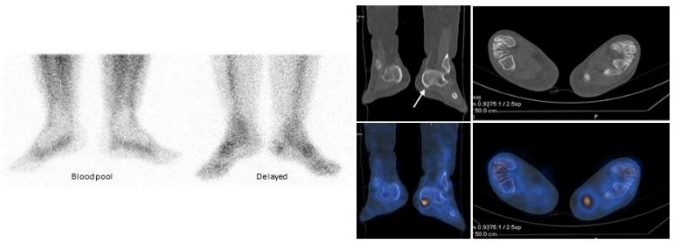

Figure 7. Plantar fasciitis of the left foot

Cuboid pulley lesion in a 49-year-old patient with chronic midfoot pain. Increased tracer uptake corresponds to focal mechanical stress at the lateroplantar ridge of the cuboid, where the peroneus longus tendon changes direction [Figure 8].[4]

Sinus tarsi syndrome[1] demonstrating increased ^{99m}Tc-MDP uptake with corresponding MRI abnormalities localized to the sinus tarsi region. Sinus tarsi syndrome is characterized by pain and tenderness in the lateral hindfoot, most commonly related to subtalar instability following ankle sprains, although nontraumatic factors may also contribute [Figure 9].[5]

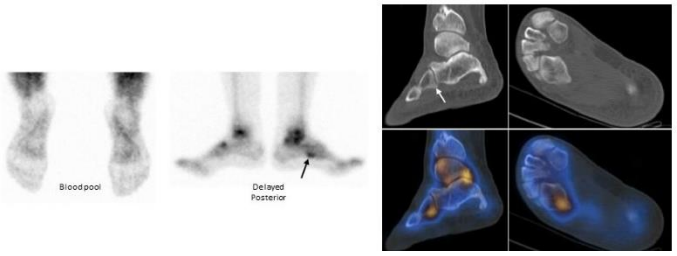

Figure 8. Cuboid pulley lesion in a patient with chronic foot pain

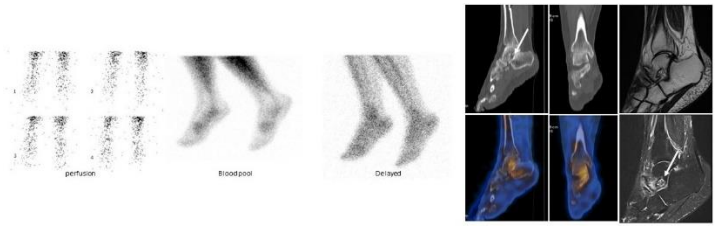

Figure 9. Sinus tarsi syndrome demonstrating increased MDP uptake with corresponding MRI changes localized to the sinus tarsi region

Reflex sympathetic dystrophy (complex regional pain syndrome) demonstrates either increased [Figure 10A] or decreased [Figure 10B] radiotracer uptake in the juxta-articular regions. CT shows osteopenic changes, and MRI reveals patchy bone marrow edema.[6,7]

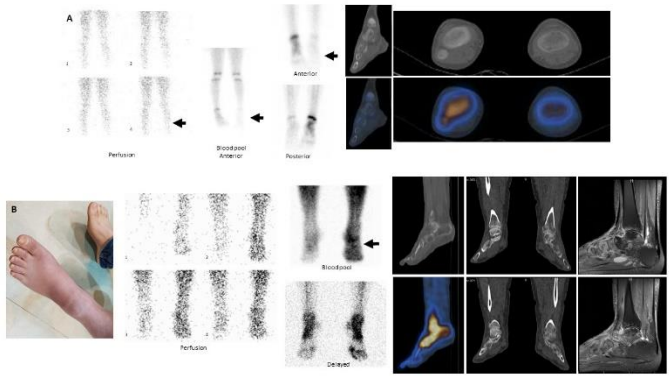

Figure 10. Reflex sympathetic dystrophy showing (A) increased and (B) decreased radiotracer uptake in juxta-articular regions

Aneurysmal bone cysts involving the calcaneus [Figure 11A] and the first metatarsal [Figure 11B]. These lesions appear as expansile, lytic lesions with thin sclerotic margins and internal septations on radiography and CT; MRI demonstrates characteristic fluid–fluid levels. Bone scintigraphy shows hypervascularity with intense delayed-phase tracer uptake. SPECT/CT improves lesion localization and assists in differentiation from aggressive lesions.[8]

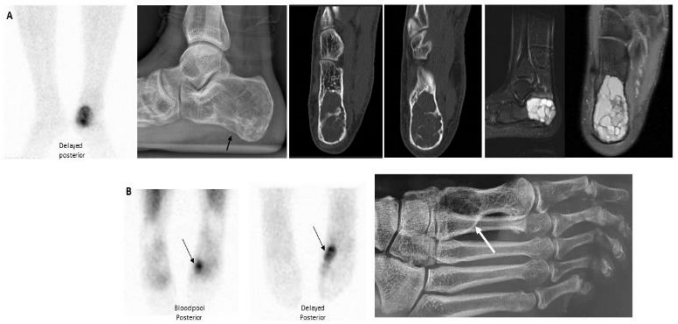

Figure 11. Aneurysmal bone cysts involving the (A) calcaneus and (B) first metatarsal

Chondroblastoma of the talus in a young patient. A rare benign cartilaginous tumor, typically arising in the epiphysis of long bones. Bone scintigraphy demonstrates intense tracer uptake, reflecting high vascularity and osteoblastic activity [Figure 12].[9]

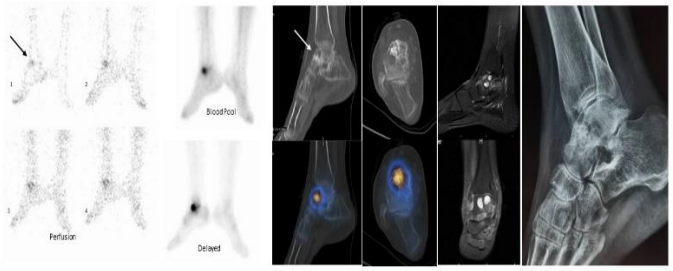

Figure 12. Chondroblastoma of the talus

Osteochondroma of the distal tibial metaphysis in a 12-year-old patient with hereditary multiple osteochondromas (HMO) [Figure 13]. MDP uptake is observed at the osseous stalk, whereas the cartilaginous cap appears photopenic. Bone scintigraphy helps screen for polyostotic involvement and potential complications.[10]

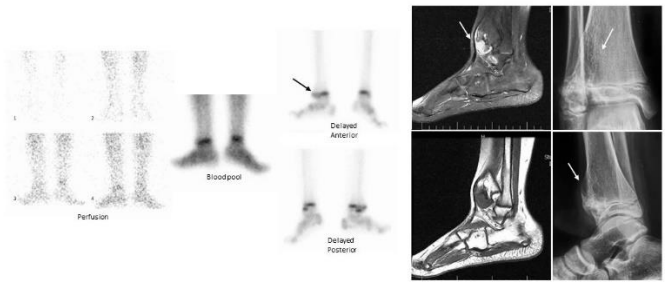

Figure 13. Osteochondroma (exostosis) of the tibia in a patient with a known history of hereditary multiple exostoses

Fibrous dysplasia involving the talus and femur in a 32-year-old patient with polyostotic disease [Figure 14]. Bone scintigraphy highlights metabolically active lesions, and bisphosphonate therapy has been shown to reduce pain and fracture risk.[11]

Figure 14. Fibrous dysplasia of the talus in a patient with known multifocal disease

Paget's disease of the calcaneus in a 67-year-old man, demonstrating intense ^99mTc-MDP uptake on both blood-pool and delayed-phase images of bone scintigraphy. Corresponding SPECT/CT reveals coarse trabeculation and cortical thickening [Figure 15]. Bone scintigraphy is highly sensitive for detecting metabolically active lesions, assessing disease extent, and monitoring therapeutic response, and it complements conventional radiography.[12,13]

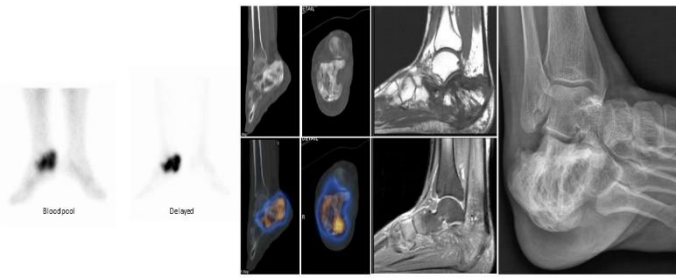

Figure 15. Paget's disease of the calcaneus

Giant cell tumor of the fifth metatarsal in a 39-year-old man, presenting as an eccentric lytic lesion with cortical thinning and expansion and demonstrating increased tracer uptake in all phases of a three-phase bone scan [Figure 16]. However, in some cases, bone scintigraphy may show only mild focal uptake and may underestimate the true extent of the tumor and any extraosseous involvement.[14]

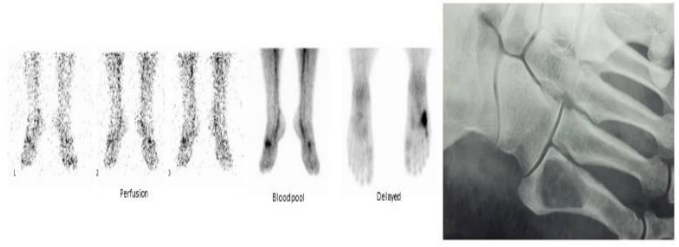

Figure 16. Giant cell tumor of the fifth metatarsal

Non-ossifying fibroma of the tibia in a 13-year-old girl. A

well-defined, eccentric metaphyseal lesion with a scalloped sclerotic rim. Bone scintigraphy shows mild-to-moderate tracer uptake in active lesions and faint uptake in healed lesions [Figure 17].[15]

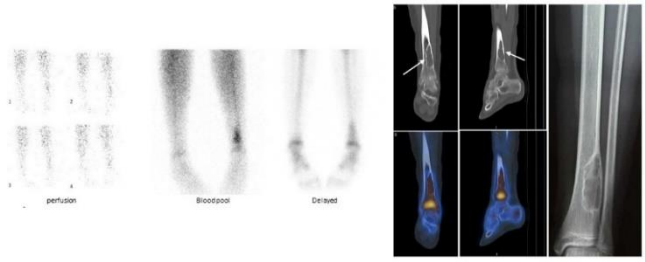

Figure 17. Non-ossifying fibroma of the tibia

Osteoid osteoma in four patients presenting with pain, demonstrating focal increased radiotracer uptake on blood-pool and delayed-phase images, with identification of a nidus on SPECT/CT. Lesions were located in the third metatarsal [Figure 18A], talus [Figure 18B], medial cuneiform [Figure 18C], and first phalanx [Figure 18D]. Osteoid osteoma is a benign, painful osteoblastic tumor that predominantly affects young patients. Hybrid imaging facilitates image-guided ablation or surgical excision.[16-18]

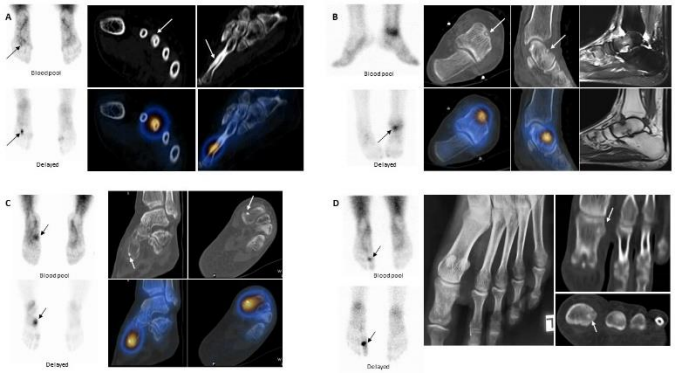

Figure 18. Osteoid osteoma involving the (A) third metatarsal, (B) talus, (C) medial cuneiform, and (D) first phalanx

Familial multiple lipomatosis involving the ankle and foot bones in a 17-year-old patient referred for evaluation of suspected osteomyelitis due to foot pain and fever [Figure 19].

Figure 19. Familial multiple lipomatosis involving the ankle and foot bones

Melorheostosis in a 12-year-old patient with pelvic and foot pain. Characteristic “dripping candle wax” cortical thickening is evident; tracer uptake varies according to disease activity. ^18F-NaF PET can detect subtle lesions, and management is primarily supportive [Figure 20].[19]

Figure 20. Melorheostosis in a patient presenting with pelvic and foot pain

Chondrosarcoma of the third proximal phalanx in a 54-year-old patient. A mixed lytic–sclerotic lesion with ring-and-arc calcifications; bone scintigraphy demonstrates increased metabolic activity, aiding lesion detection and treatment planning [Figure 21].[20]

Figure 21. Chondrosarcoma of the third proximal phalanx

Ewing sarcoma of the third metatarsal in a 22-year-old patient. Cortical destruction with associated soft-tissue involvement is observed; bone scintigraphy assists in staging and complements MRI and histopathologic evaluation [Figure 22].[21]

Figure 22. Ewing sarcoma of the third metatarsal

Metastases to the calcaneus and fibula in a 47-year-old patient with colon cancer. Bone scintigraphy demonstrates distal lower extremity metastases, which are relatively uncommon, aiding in detection and differentiation from benign lesions [Figure 23].[22-24]

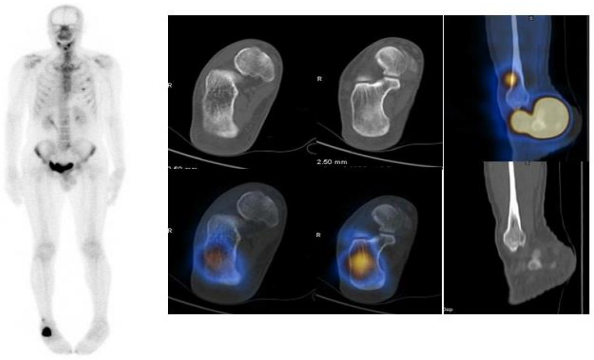

Figure 23. Metastatic involvement of the calcaneus and fibula

Osteosarcoma of the fourth phalanx. A moth-eaten lytic lesion with a sunburst periosteal reaction and intense focal tracer uptake on bone scintigraphy; SPECT/CT or MRI confirms the extent of disease and detects metastatic involvement [Figure 24].[13,25]

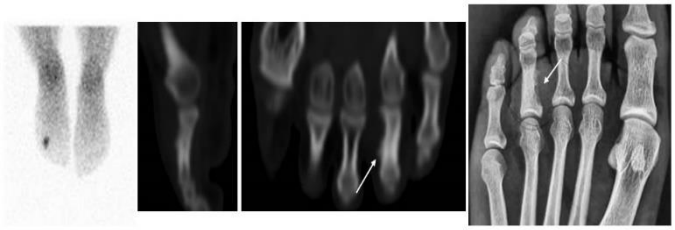

Figure 24. Osteosarcoma of the fourth phalanx

Avascular necrosis of the foot involving the navicular (Köhler disease) [Figure 25A], post-traumatic talus [Figure 25B], and second metatarsal head (Freiberg disease) [Figure 25C]. Photopenic "cold spots" with surrounding hyperemia are observed on bone scintigraphy; imaging is most useful 7–10 days after ischemia and serves as a complement to MRI.[26]

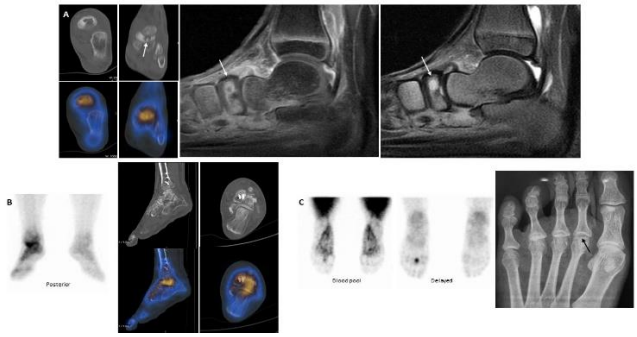

Figure 25. (A) Navicular AVN (Köhler disease); (B) post-traumatic talar AVN; (C) second metatarsal head AVN (Freiberg disease)

Infectious and inflammatory conditions include tibiotalar arthritis [Figure 26A], medial cuneiform osteomyelitis [Figure 26B], chronic calcaneal osteomyelitis [Figure 26C], and fifth metatarsal osteomyelitis [Figure 26D]. MRI demonstrates periosteal reaction and bone marrow edema. In contrast, early-phase hyperemia and delayed-phase focal tracer uptake on bone scintigraphy are valuable for evaluating and excluding osteomyelitis, particularly in patients with diabetic foot.[27]

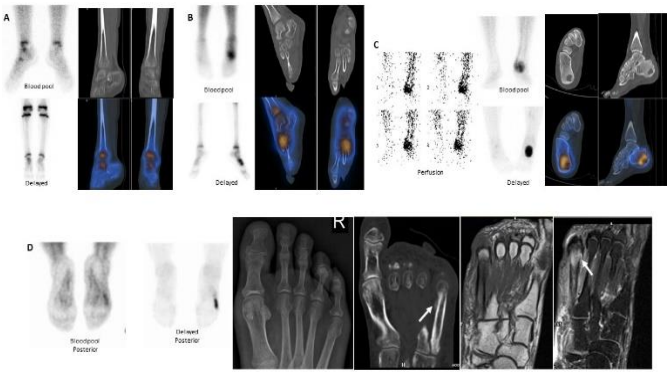

Figure 26. (A) tibiotalar arthritis, (B) osteomyelitis of the medial cuneiform, (C) chronic active osteomyelitis of the calcaneus, and (D) osteomyelitis of the fifth metatarsal

Results

SPECT/CT improved lesion localization and characterization within the anatomically complex ankle–foot region. Characteristic uptake patterns were observed in fractures, osteochondral lesions, inflammatory conditions, avascular necrosis, benign and malignant bone tumors, and less common entities. Recognition of normal variants, such as accessory ossicles and bipartite sesamoids, was essential to avoid misinterpretation.

Discussion

The diverse pathologies of the ankle and foot illustrate how nuclear medicine, particularly 99mTc-MDP SPECT/CT, enhances diagnostic precision in anatomically complex cases. Beyond detecting increased osteoblastic activity, SPECT/CT enables correlation of functional abnormalities with precise anatomical localization, which is critical in regions composed of small, overlapping bones. This approach not only improves differentiation between symptomatic and incidental findings—such as accessory ossicles or bipartite sesamoids—but also facilitates assessment of lesion activity and extent, including fractures, osteochondral defects, and benign or malignant tumors.[28,29] Moreover, bone scintigraphy provides distinct value in early-stage or subtle conditions that may not be readily apparent on radiography or MRI, such as avascular necrosis, stress fractures, or inflammatory syndromes.30,31 Recognition of disease-specific uptake patterns and normal variants is essential to prevent misdiagnosis. In infectious processes, for example, the combination of early-phase hyperemia and delayed-phase tracer uptake supports diagnosis;

however, correlation with MRI and clinical findings remains necessary because of limited specificity.[27] Importantly, SPECT/CT contributes to preoperative planning and follow-up of both benign and malignant lesions by accurately delineating lesion extent and activity.

Conclusion

^{99m}Tc-MDP planar scintigraphy and SPECT/CT are valuable imaging modalities for evaluating ankle and foot pathologies, aiding lesion localization, characterization, and treatment planning. Recognition of normal variants, growth-related tracer uptake, and characteristic disease-specific patterns enhances diagnostic accuracy and supports optimal patient management in musculoskeletal nuclear medicine.

Acknowledgement

N/A

Authors Contribution: Authors who conceived and designed the analysis: Ramin Sadeghi (RS), Authors who collected the data: Ramin Sadeghi (RS), Alireza Mousavian (AM), Authors who contributed data or analysis tools: Alireza Mousavian (AM), Vahid Reza Dabbagh Kakhki (VDK), Authors who performed the analysis: Ramin Sadeghi (RS), Pegah Sahafi (PS), Authors who wrote the paper: Pegah Sahafi (PS), Mohammad Hadi Samadi (MHS)

Declaration of Conflict of Interest: The authors do NOT have any potential conflicts of interest for this manuscript.

Declaration of Funding: The authors received NO financial support for the preparation, research, authorship, and publication of this manuscript.

Declaration of Ethical Approval for Study: Ethical approval was not required for this case series in accordance with institutional guidelines.

Declaration of Informed Consent: No identifiable patient information (names, initials, hospital identification numbers, or photographs) is included in this manuscript.

Pegah Sahafi MD[1]
Mohammad Hadi Samadi MD[1]
Alireza Mousavian MD[2]
Vahid Reza Dabbagh Kakhki MD[1]
Ramin Sadeghi MD1[1]

1 Nuclear Medicine Research Center, Mashhad University of Medical Science, Mashhad, Iran
2 Orthopedic Research Center, Mashhad University of Medical Sciences, Mashhad, Iran

References

1. Achong DM. Unsuspected accessory ossicle in possible sinus tarsi syndrome: the value of bone SPECT/CT. Clin Nucl Med. 2020;45(4):e215-e216. doi: 10.1097/RLU.0000000000002943.
2. Huang J, Servaes S, Zhuang H. Os trigonum syndrome on bone SPECT/CT. Clin Nucl Med. 2014;39(8):752-754. doi: 10.1097/RLU.0000000000000434.
3. Wang C-C, Yang K-C, Chen H. Current treatment concepts for osteochondral lesions of the talus. Tzu Chi Med J. 2020;33(3):243-249. doi: 10.4103/tcmj.tcmj_106_20.
4. Chang M-Y, Hong SH, Yoo HJ, Choi J-Y, Chae H-D, Moon SJ. MRI of the cuboid pulley lesion. AJR Am J Roentgenol. 2018;211(4):867-871. doi: 10.2214/AJR.17.19497.
5. Mahato A, Mukherjee PB, Jha DK, Pandit A. Sinus Tarsi Syndrome: Diagnosed on 99mTc-MDP bone SPECT/CT. Asia Ocean J Nucl Med Biol. 2020;8(2):153-156. doi: 10.22038/AOJNMB.2020.45897.1309.
6. Hod N, Horne T. Decreased uptake on 3-phase bone scintigraphy in posttalar fracture reflex sympathetic dystrophy. Clin Nucl Med. 2004;29(9):560-561. doi: 10.1097/01.rlu.0000134983.24257.26.
7. Kwon HW, Paeng JC, Nahm FS, et al. Diagnostic performance of three-phase bone scan for complex regional pain syndrome type 1 with optimally modified image criteria. Nucl Med Mol Imaging. 2011;45(4):261-267. doi: 10.1007/s13139-011-0104-x.
8. Hudson T. Scintigraphy of aneurysmal bone cysts. AJR Am J Roentgenol. 1984;142(4):761-765. doi: 10.2214/ajr.142.4.761.
9. Humphry A, Gilday DL, Brown RG. Bone scintigraphy in chondroblastoma. Radiology. 1980;137(2):497-499. doi: 10.1148/radiology.137.2.6449026.
10. Murphey MD, Choi JJ, Kransdorf MJ, Flemming DJ, Gannon FH. Imaging of osteochondroma: variants and complications with radiologic-pathologic correlation. Radiographics. 2000;20(5):1407-1434. doi: 10.1148/radiographics.20.5.g00se171407.
11. Parekh SG, Donthineni-Rao R, Ricchetti E, Lackman RD. Fibrous dysplasia. J Am Acad Orthop Surg. 2004;12(5):305-313. doi: 10.5435/00124635-200409000-00005.
12. Duch J, Fuster D, Ortín J, Setoain X, Pons F. Bilateral

Paget disease of the calcaneus diagnosed by conventional bone scintigraphy. Clin Nucl Med. 2006;31(12):808-809. doi: 10.1097/01.rlu.0000247783.43949.c1.

13. DE WAELE S, Lonneux M, Vande Berg B, Nzeusseu A, Brasseur J-P, Lecouvet FE. Paget disease and osteosarcoma of the calcaneus. Clin Nucl Med. 2001;26(3):244-246. doi: 10.1097/00003072-200103000-00018.
14. Levine E, De Smet AA, JR N, Martin NL. Scintigraphic evaluation of giant cell tumor of bone. . AJR Am J Roentgenol. 1984;143(2):343-348. doi: 10.2214/ajr.143.2.343.
15. Hod N, Levi Y, Fire G, et al. Scintigraphic characteristics of non-ossifying fibroma in military recruits undergoing bone scintigraphy for suspected stress fractures and lower limb pains. Nucl Med Commun. 2007;28(1):25-33. doi: 10.1097/MNM.0b013e328012e3de.
16. Sahafi P, Sadeghi R, Mousavian A. A Rare Case of Osteoid Osteoma of the Medial Cuneiform Bone at Tibialis Anterior Insertion Confirmed by Bone Scan SPECT/CT. Clin Nucl Med. 2024 ;49(12) doi: 10.1097/RLU.0000000000005497.
17. Samadi MH, Khezri S, Soltani S, Dalooei SMAS, Aghaee A. A Rare Case of Osteoid Osteoma of the Distal Physis of the Fibula Confirmed by Bone SPECT/CT Scanning. Clin Nucl Med. 2025;50(8):778-780. doi: 10.1097/RLU.0000000000005765.
18. Farid K, El-Deeb G, Vigneron NC. SPECT-CT improves scintigraphic accuracy of osteoid osteoma diagnosis. Clin Nucl Med. 2010;35(3):170-171. doi: 10.1097/RLU.0b013e3181cc648f.
19. Gholamrezanezhad A. Bone scintigraphy elucidates different metabolic stages of melorheostosis. Pan Afr Med. 2012;11(1). doi: 10.11604/pamj.2012.11.21.686.
20. Choi WH, Han EJ, Chang KB, Joo MW. Quantitative SPECT/CT for differentiating between enchondroma and grade I chondrosarcoma. Sci Rep. 2020;10(1):10587. doi: 10.1038/s41598-020-67506-4.
21. Ozaki T. Diagnosis and treatment of Ewing sarcoma of the bone: a review article. J Orthop Sci. 2015;20(2):250-263. doi: 10.1007/s00776-014-0687-z.
22. Singh C, Gupta M, Singh J, Ali A. Isolated calcaneal metastasis: an unusual presentation of lung carcinoma as heel pain. Clin Nucl Med. 2016;41(3):214-216. doi: 10.1097/RLU.0000000000001064.
23. Li W, Li W, Zhang R. Metastasis to the medial cuneiform bone from squamous cell carcinoma of the lung revealed by bone Scintigraphy. Clin Nucl Med. 2016;41(12):946-947. doi: 10.1097/RLU.0000000000001373.
24. Bahrabadi M, Otoukesh B, Moghtadaei M, Hoseinzadeh S, Amiri S. Foot metastasis: review of 38 cases. ABJS. 2021;9(1):122. doi: 10.22038/abjs.2020.49792.2474.
25. Suthar R, Bharwani N, Pareek P, et al. Role of bone scintigraphy (bone scan) in skeletal osteosarcoma: A retrospective audit and review from tertiary oncology centre. J Orthop. 2024;48:20-24. doi: 10.1016/j.jor.2023.11.038.
26. Ng FH, Lai TKB, Lam SY, Pan NY, Luk WH. Hybrid magnetic resonance imaging with single photon emission computed tomography/computed tomography bone scan for diagnosis of avascular necrosis of femoral head. J Clin Imaging Sci. 2021;11:2. doi: 10.25259/JCIS_205_2020.
27. Llewellyn A, Kraft J, Holton C, Harden M, Simmonds M. Imaging for detection of osteomyelitis in people with diabetic foot ulcers: A systematic review and meta-analysis. Eur J Radiol. 2020;131:109215. doi: 10.1016/j.ejrad.2020.109215.
28. Gnanasegaran G, Cook G, Adamson K, Fogelman I. Patterns, variants, artifacts, and pitfalls in conventional radionuclide bone imaging and SPECT/CT. Elsevier; 2009;39(6):380-395. doi: 10.1053/j.semnuclmed.2009.07.003.
29. Palmedo H, Marx C, Ebert A, et al. Whole-body SPECT/CT for bone scintigraphy: diagnostic value and effect on patient management in oncological patients. Eur J Nucl Med Mol Imaging. 2014;41(1):59-67. doi: 10.1007/s00259-013-2532-6.
30. Ikeda T, Kitajima K, Tsuchitani T, Takahashi Y, Hama Y, Kotura N. Effectiveness of quantitative bone SPECT/CT for bone metastasis diagnosis. Hell J Nucl Med. 2022;25(3):253-259. doi: 10.1967/s002449912513.
31. Flaherty A, Tomlinson E, Weaver B, et al. Factors Associated with Non-Unions of Fifth Metatarsal Fractures. Arch Bone Jt Surg. 2025;13(6):367-377. doi: 10.22038/ABJS.2025.81228.3708. PMID: 40641895; PMCID: PMC12238859.